PHILOSOPHICAL TRANSACTIONS OF THE ROYAL SOCIETY B BIOLOGICAL SCIENCES

Foveate vision in deep–sea teleosts: a comparison of primary visual and olfactory inputs

Shaun P. Collin, Darren J. Lloyd and Hans Joachim Wagner

Phil. Trans. R. Soc. Lond. B 2000 **355**, 1315-1320
doi: 10.1098/rstb.2000.0691

THE ROYAL SOCIETY

doi 10.1098/rstb.2000.0691

Foveate vision in deep-sea teleosts: a comparison of primary visual and olfactory inputs

Shaun P. Collin[1]* Darren J. Lloyd[1] and Hans-Joachim Wagner[2]

[1]*Department of Zoology, The University of Western Australia, Nedlands 6907, Western Australia, Australia*
[2]*Anatomisches Institut, Eberhard-Karls-Universität Tübingen, Österbergstrasse 3, D-72074 Tübingen, Germany*

The relative importance of vision in a foveate group of alepocephalid teleosts is examined in the context of a deep-sea habitat beyond the penetration limits of sunlight. The large eyes of *Conocara* spp. possess deep convexiclivate foveae lined with Müller cells comprising radial shafts of intermediate filaments and horizontal processes. Photoreceptor cell (171.8×10^3 rods mm^{-2}) and retinal ganglion cell (11.9×10^3 cells mm^{-2}) densities peak within the foveal clivus and the perifoveal slopes, respectively, with a centro-peripheral gradient between 3:1 (photoreceptors) and over 20:1 (ganglion cells). The marked increase in retinal sampling localized in temporal retina, coupled with a high summation ratio (13:1), suggest that foveal vision optimizes both spatial resolving power and sensitivity in the binocular frontal visual field. The elongated optic nerve head is comprised of over 500 optic papillae, which join at the embryonic fissure to form a thin nervous sheet behind the eye. The optic nerve is divided into two axonal bundles; one receiving input from the fovea (only unmyelinated axons) and the other from non-specialized retinal regions (25% of axons are myelinated), both of which appear to be separated as they reach the visual centres of the central nervous system. Comparison of the number of primary (first-order) axonal pathways for the visual (a total of 63.4×10^6 rod photoreceptors) and olfactory (a total of 15.24×10^5 olfactory nerve axons) inputs shows a marked visual bias (ratio of 41:1). Coupled with the relative size of the optic tecta (44.0 mm^3) and olfactory bulbs (0.9 mm^3), vision appears to play a major role in the survival of these deep-sea teleosts and emphasizes that ecological and behavioural strategies account for significant variation in sensory brain structure.

Keywords: retina; fovea; optic nerve; olfactory nerve; optic tectum; retinal ganglion cells

1. INTRODUCTION

The retinae of shallow-water teleosts boast a remarkably diverse range of retinal specializations including localized increases in cell density (ganglion cells and photoreceptors) in various retinal regions (Collin 1999). These regions of increased density provide higher sampling, and therefore increased spatial resolving power, for particular regions of the visual field. An area centralis subtends a specific region of the visual field while a streak subtends a wider, panoramic visual field. A retinal pit or fovea can also be associated with an area centralis and, on examination of 42 species of teleosts, four foveal types have been identified on structural criteria (Collin & Collin 1999).

In shallow water, the need for higher spatial resolving power and the optical advantages afforded by the fovea (such as image magnification, the detection and maintenance of accurate fixation, monocularly mediated directional focus and the perception of depth) suggest that the importance of vision in foveate species is relatively high and that this specialized sampling may be reflected centrally. The foveate bass, *Paralabrax* spp., provides an excellent example where the representation of a temporal convexiclivate fovea with a marked increase in retinal ganglion cell density is magnified five times within the contralateral optic tectum (Schwassmann 1975).

Although the presence of foveae in the retinae of deep-sea teleosts seems counter-intuitive given the low levels of sunlight, considered visually irrelevant below 1000 m, there are, in fact, over 30 species of deep-sea teleosts known to possess foveae, most of which are represented within the family Alepocephalidae. Species within the genus *Conocara* have received particular attention, where a deep foveal pit located in the temporal retina is lined with radial fibres (Müller cells) and possesses a centro-peripheral gradient of retinal ganglion cells of up to 37:1 (Locket 1992; Collin & Partridge 1996; Wagner *et al.* 1998). Although the refractive index of the Müller cell lining needs to be measured, its thickness and staining properties suggest it may refract light, distorting or magnifying the image of an object passing over the fovea. Assuming that the eyes remain fixed in the head, this distortion could produce a skewed image, providing a useful cue about depth perception and a method of breaking luminescent camouflage (Locket 1985).

*Author and address for correspondence: Department of Anatomical Sciences, The University of Queensland, Brisbane, Queensland 4072, Australia (s.collin@mailbox.uq.edu.au).

PHILOSOPHICAL TRANSACTIONS OF THE ROYAL SOCIETY B BIOLOGICAL SCIENCES

The presence of large eyes possessing a fovea in *Conocara* spp. suggests that vision is an important sensory modality in this group of deep-sea fishes, despite the fact that all the members of this group survive beyond the penetration limits of sunlight. In order to assess the relative importance of vision in these foveate deep-sea teleosts, we examine foveal structure and the centro-peripheral gradients of both ganglion and photoreceptor cells in two species (*Conocara macroptera* and *Conocara murrayi*) collected from depths of between 1400 and 2900 m. The number of primary (first-order) optic (rod photoreceptors) and olfactory (olfactory nerve axons) inputs and the relative size of the optic tecta and the olfactory bulbs is also compared. Large eye size, a localized increase in retinal sampling within the foveal region, the presence of myelinated optic axons within the retina and the large size of the optic tecta, suggest that visually complex behaviours, at least with respect to olfaction, play a major sensory role in this group of teleosts.

2. FOVEAL RETINAL SAMPLING

The large eyes of *C. macroptera* and *C. murrayi* are supported by cartilaginous optic pedicels or eyestalks, which are anchored to the base of the cranium and inserted rostral to the olfactory bulbs. Although possessing the full complement of extraocular eye muscles, the eyes fill the orbit, leaving little space for extensive eye movements. The pupil is rostrally tapered, leaving a nasal aphakic gap, where light entering the eye will not be focused by the spherical lens. Assuming that eye movements are minimal, ophthalmoscopic examination of the visual field in *C. macroptera* shows that each eye possesses a large monocular visual field of *ca.* 185° (15° from the dorsal vertical axis to 20° beyond the ventral vertical axis). A binocular overlap of 40° extends from 30° ventral of the caudal horizontal axis to 20° dorsal of the rostral horizontal axis.

The foveal pit in both *C. macroptera* and *C. murrayi* lies in the temporal retina at the end of an elongated optic nerve. The nerve inserts into the embryonic fissure and terminates close to the ventro-nasal retinal margin (figure 1*a*). The foveal pit is lined by a thick layer of cell processes emanating from radially orientated Müller cells that occupy 25% of the retinal thickness (figure 1*c–f*). The radial columns of the darkly staining Müller cells vary in thickness between 6 μm (30 cm standard length *C. macroptera*) and 16 μm (52 cm standard length *C. murrayi*) near the inner limiting membrane and are composed of what appear to be dense aggregations of intermediate filaments (8–10 nm in diameter, figure 1*d*). These give rise to horizontally directed processes, which reach 70 nm in diameter and form dense multistack complexes in foveal and perifoveal regions (figure 1*f*). In non-foveal retina, the Müller cell endfeet lining the inner limiting membrane are appreciably thinner, where the horizontally directed cell processes are lost and replaced by granular cytoplasm.

Using a whole-mount technique (Collin & Pettigrew 1988), topographic analysis of both the photoreceptor and ganglion cell distributions were found to peak within the foveal region with a centro-peripheral gradient between 3:1 (photoreceptors) and over 20:1 (ganglion cells). However, while the peak photoreceptor density (171.8×10^3 rods mm^2) lies at the base of the foveal clivus, the peak ganglion cell density (11.9×10^3 cells mm^{-2}) lies in the perifoveal region with no ganglion cells located within the centre of the pit (figure 1*a*,*b*). In addition, the foveal pit is not symmetrically circular but tapers dorsally for a length of 150 μm.

Assuming the period of the cell spacing within the perifoveal region subtends the minimum separable angle (MSA), measurements of spatial resolving power or visual acuity provide different values for the photoreceptor and ganglion cell arrays. In the perifoveal region of *C. macroptera*, the MSA varies from 1.8 minutes of arc (calculated using photoreceptor spacing; Tamura 1957) to 5.8 minutes of arc (calculated using ganglion cell spacing; Collin & Pettigrew 1989) in a 30 cm individual. The differences in photoreceptor and ganglion cell density convert to a summation ratio (photoreceptor to ganglion cell input) of 13:1 within this region, compared to 44:1 in peripheral (non-specialized) retina. Therefore, although there is a relatively large summation ratio within the perifoveal region (at least when compared to foveate shallow-water species, which may have a ratio as little as 1:1; Nicol 1989), this increase in sensitivity is balanced by a high centro-peripheral gradient to optimize increased spatial resolving power.

A large retinal area (a maximum of 755 mm^3 in the six specimens examined) predicts a high number of ganglion cells (and therefore axons comprising the optic nerve). In the largest of each species, 13.6×10^5 cells (30 cm standard length *C. macroptera*) and 7.3×10^5 cells (52 cm standard length *C. murrayi*) were found within the ganglion cell layer. Although these high numbers of axons reflect high spatial sampling, over 97% of the retinal area in each species is occupied by relatively low ganglion cell densities between 0.6 and 3.0×10^3 cells mm^{-2}, leaving 3% of the retinal area dedicated to foveal vision. Therefore, in the absence of any other retinal landmarks, it may be assumed that the position of the fovea aligns the visual axis, which would lie in the lower frontal visual field in these two species.

3. AXONAL MYELINATION WITHIN THE RETINAL NERVE FIBRE LAYER

Analysis of ultrathin sections cut perpendicular to the course of the ganglion cell axons surrounding the fovea in temporal retina show a large proportion (*ca.* 25%) of the ganglion cell axons within the retina are myelinated. Up to six cellular (glial) processes loosely wrap these large diameter fibres, which are interspersed among large numbers of unmyelinated axons (figure 2*a–d*). Although the myelinated and unmyelinated axons form bundles or fascicles divided by Müller cells, there does not seem to be any retinal order in the position of the myelinated axons with respect to their proximity to the inner limiting membrane. The foveal region (within a radius of 0.5 mm from the centre of the pit) does not possess myelinated axons.

Easter *et al.* (1984) consider the myelinated axons in the retinal fibre layer of the goldfish to belong to the largest and oldest ganglion cells, which lie within the deeper

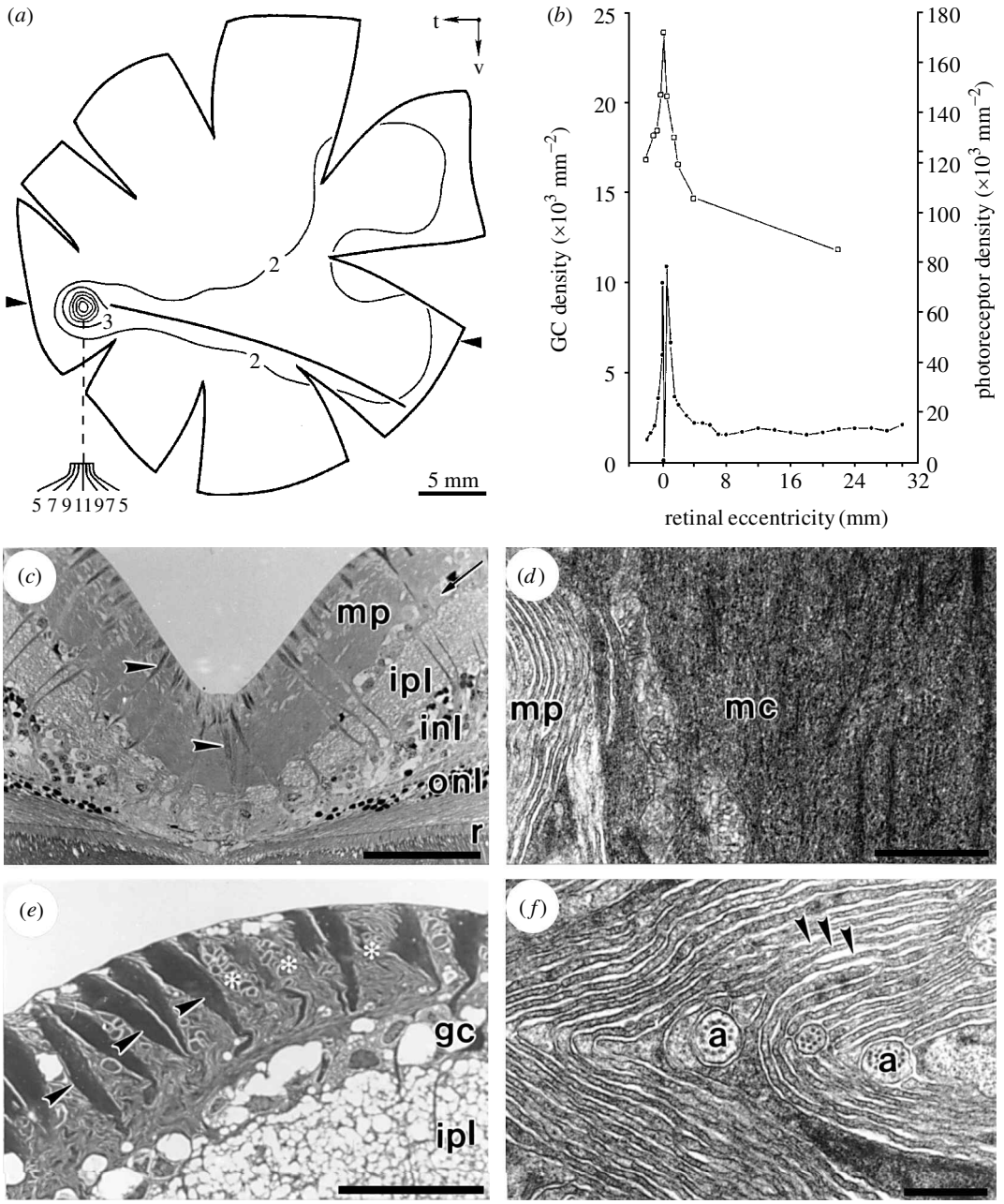

Figure 1. (*a*) Topographic distribution of retinal ganglion cells in *C. macroptera* showing a localized increase in density in the perifoveal region of the temporal retina. All densities are $\times 10^3$ cells mm^{-2} with the peak density reaching 11 900 cells mm^{-2}. Note the elongated optic nerve extending across ventral retina. (*b*) Temporo-nasal density profile (between the arrowheads in (*a*)) of both photoreceptor (empty squares) and ganglion cell (black circles) populations in *C. macroptera*. Note the lack of ganglion cells in the foveal pit. (*c*) Transverse section of the foveal pit in *C. macroptera* showing the lining of Müller cell processes (mp) interrupted by radial columns (arrowheads). An arrow depicts the level of the ganglion cell layer. (*d*) Electron micrograph of the radial column of a Müller cell (mc), which gives rise to complexes of fine processes (mp) in *C. murrayi*. (*e*) Light micrograph of the perifoveal slope in *C. murrayi*, showing its Müller cell lining with large radial columns (arrowheads) and radial processes (asterisks). (*f*) High-power electron micrograph of the Müller cell processes (arrowheads) surrounding a number of unmyelinated axons (a). gc, ganglion cell layer; inl, inner nuclear layer; ipl, inner plexiform layer; onl, outer nuclear layer; r, rod photoreceptors; v, ventral. Scale bars, (*c*) 100 µm; (*d*) 0.5 µm; (*e*) 50 µm; (*f*) 0.1 µm.

(sclerad) regions of the retina. The identification of unmyelinated profiles along the inner limiting membrane also suggests that the unmyelinated axons in this region belong to the youngest ganglion cells, which are generated in the retinal periphery. This age-related order of myelinated and unmyelinated axons within the retina does not appear to hold for *Conocara* spp., at least in close proximity to the fovea and the elongated optic nerve, although the proximity of our sampled foveal tissue to the temporal periphery may preclude an ordered subdivision of axons. Clearly, a more thorough topographic examination of axonal myelination will confirm any ordered retinotopicity, but given the unique arrangement of multiple optic papillae along the length of the elongated optic nerve head (see § 4 below), the cues for axonal guidance and retinal growth may differ.

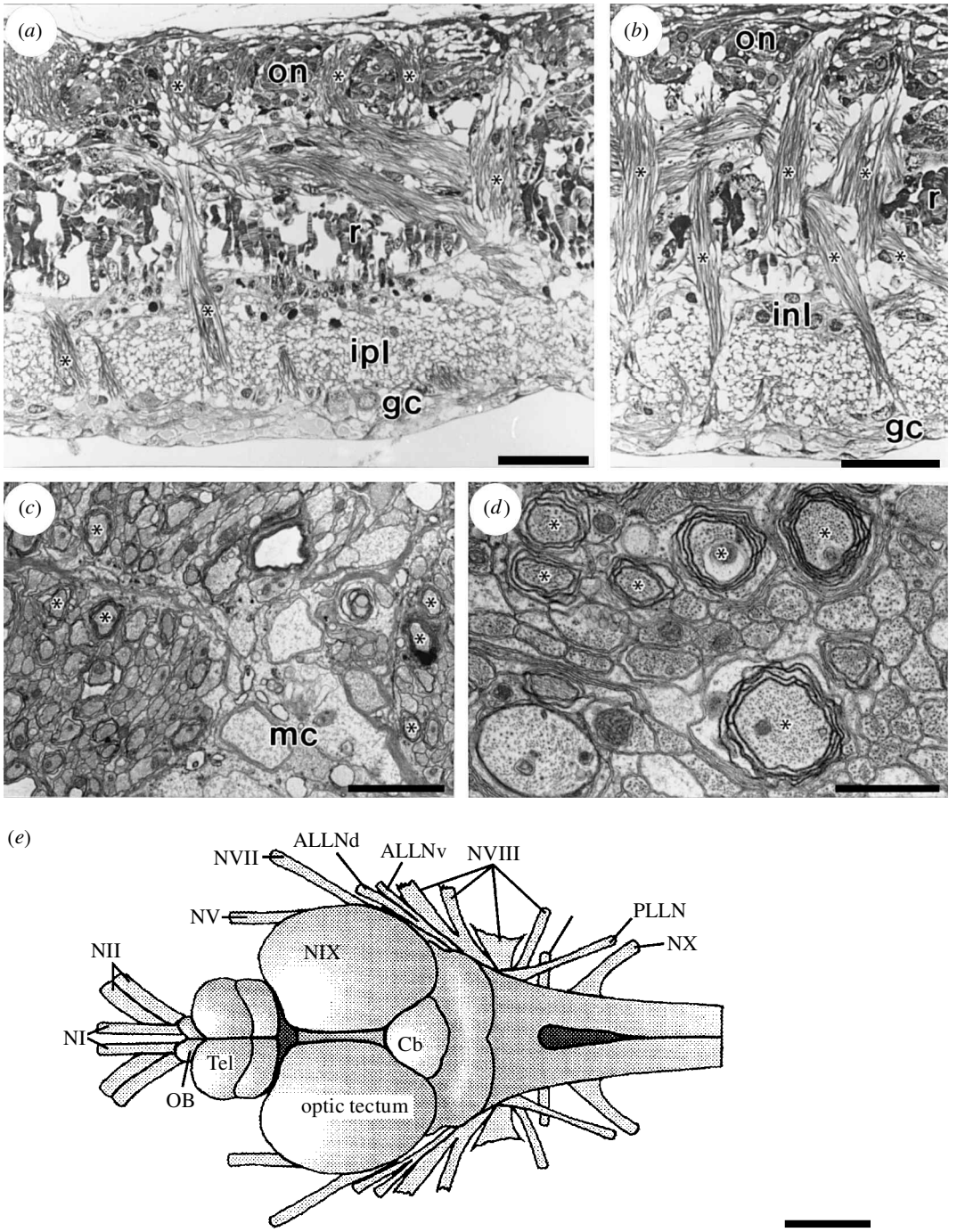

Figure 2. (*a*) Light micrograph of a retinal section of *C. murrayi* cut parallel to the plane of the embryonic fissure, where the elongated optic nerve (on) is formed by a series of axonal papillae (asterisks). (*b*) Higher power of a complex of axonal papillae (asterisks). Note that some axonal bundles traverse the retina horizontally and join other papillae. (*c*) Electron micrograph of the optic nerve fibre layer in a transverse section of central retina showing the different appearance of the Müller cells (mc) and a number of myelinated axon profiles (asterisks) in *C. murrayi*. The inner limiting membrane is towards the bottom of the micrograph. (*d*) Higher power of the large number of myelinated axons (asterisks) with loose glial wrapping. (*e*) Camera lucida drawing of a dorsal view of the brain and cranial nerves in *C. macroptera*. Note the relatively large size of the optic tecta in comparison to the olfactory bulbs (OB). ALLNd, dorsal division of the anterior lateral line nerve; ALLNv, ventral division of the anterior lateral line nerve; Cb, cerebellum; gc, ganglion cell layer; inl, inner nuclear layer; ipl, inner plexiform layer; NI, olfactory nerve; NII, optic nerve; NV, trigeminal nerve; NVII, facial nerve; NVIII, octaval or vestibulocochlear nerve; NIX, glossopharangeal nerve; NX, vagus nerve; PLLN, posterior lateral line nerve; r, rod photoreceptors; tel, telencephalon. Scale bars, (*a*) 100 μm; (*b*) 50 μm; (*c*) 1 μm; (*d*) 0.3 μm; (*e*) 2 mm.

The growth-related organization of the retinal ganglion cell axons in goldfish predicts that the ganglion cells in the perifoveal region of *Conocara* spp. are new cells, presumably generated in the temporal periphery. However, localized signals must inhibit axonal myelination in the cohort of ganglion cells destined to remain within the confines of the perifoveal region in this deep-sea species. In a topographic study of the retinal ganglion

cell layer and the optic nerve in the foveate sandlance, *Limnichthyes fasciatus*, the axons of a cohort of small ganglion cells lying within the convexiclivate fovea are similarly unmyelinated and retinotopically localized in the rostral region of the optic nerve (Collin & Collin 1988).

Alternatively, myelination of the larger axons in non-foveal retinal regions may provide fast-conducting channels from the retinal ganglion cells to the visual centres of the central nervous system (CNS). A clear correlation exists between axon diameter and conduction velocity, where large axon diameters give rise to fast conduction velocities. Therefore, a subset of ganglion cells with large diameter (myelinated) axons may be fast conducting and mediate rapid orientation to bioluminescent light sources (as has been suggested for deep-sea scopelarchids, which possess a cohort of large ganglion cells; Collin *et al.* 1998) and in the maintenance of foveal fixation (Locket 1985). The myelination of the larger axons may also overcome the problem of decreased conduction velocity known to occur at low temperatures (Döving & Gemne 1965) such as those experienced in the deep sea.

4. MULTIPLE OPTIC NERVE PAPILLAE

The optic nerve in *Conocara* spp. is elongated and extends almost horizontally from the temporal fovea to the naso-ventral retinal margin along the embryonic fissure (figure 1*a*). Bundles or fascicles of retinal ganglion cell axons, often divided by Müller cells, join the optic nerve via a large series of multiple papillae (figure 2*a*,*b*). Each papilla lies *ca.* 50 µm apart and possesses thousands of axons. Lying along the length of a 30 mm optic nerve (in a 30 cm standard length individual), over 500 optic nerve papillae pool retinal input and join the optic nerve behind the retina. In some regions, the papillae seem ordered with regular insertion points into the optic nerve. However, in other areas, bundles of axons traverse from one papilla to another at either the level of the inner plexiform layer or sclerad to the photoreceptor layer (figure 2*a*,*b*).

The elongated optic nerve exits the retina along the embryonic fissure and forms two distinct nerve components beneath the sclera. The largest component is a thin sheet of nervous tissue extending from the naso-ventral retinal margin almost to the temporal fovea. A smaller, circular nerve emanates directly from temporal (foveal) retina, and is closely opposed to the edge of the nervous sheet. Distal to the scleral eyecup, both nerves become circular in profile but remain identifiably separate until they reach the CNS (figure 2*e*). Although the terminal fields of the two optic nerve components have not yet been traced, it is tempting to speculate that the smaller nerve receives foveal input while the larger nerve receives input from the remainder of the (non-specialized) retina, providing an excellent model for the study of parallel processing.

5. COMPARISON OF PRIMARY VISUAL AND OLFACTORY INPUT

With the limited prospect of electrophysiological analysis of these deep-sea fishes, the primary (first-order) visual and olfactory inputs in *C. macroptera* have been examined by assessing the total number of rod photoreceptors and olfactory nerve axons, respectively. The total population of rods was calculated by multiplying the mean rod density between each iso-density contour by its measured area, and adding these numbers together. A total of 63.4×10^6 rod photoreceptors is found to provide the maximum number of visual inputs in *C. macroptera*. The total number of olfactory nerve axons was calculated using an automated montaging system connected to a transmission electron microscope. A regular sampling (1%) of the entire olfactory nerve reveals that 15.24×10^5 unmyelinated olfactory axons are separated into bundles by ensheathing glial cells and mediate the primary olfactory input. Therefore, prior to second-order processing and convergence of sensory information, the ratio of optic to olfactory input is 41:1 further emphasizing the behavioural importance of vision in this foveate deep-sea teleost.

Morphometric comparison of the volume of the optic tecta and olfactory bulbs in *C. macroptera* using the ellipsoid model of Huber *et al.* (1997), shows that the optic tecta (44.0 mm^3) are 50 times larger than the olfactory bulbs (0.9 mm^3) (figure 2*e*). A comparable ratio exists for the visual shallow-water species *Aquidens pulcher*, that similarly possesses large optic tecta (6.1 mm^3) and small olfactory bulbs (0.2 mm^3), and possesses a ratio of 40:1 (S. P. Collin and H.-J. Wagner, unpublished data).

To our knowledge, this is the first report of a quantitative comparison of primary input from more than one sensory modality within the same individual (in shallow- or deep-water species) and, together with morphometric data of the relative size of corresponding sensory brain structures, provide an assessment of differential sensory capacity. A comparison of second-order inputs (retinal ganglion cells versus olfactory tract axons) is now required to assess the relative sensory input to the CNS.

Aspects of sensory ecology are reported to underlie differences in the development of the optic tecta (Huber & Rylander 1991) and the olfactory bulbs (Kotrschal & Palzenberger 1992) in a variety of shallow-water teleosts. In a comprehensive study of brain structure in African cichlids, Huber *et al.* (1997) suggest that visual performance is optimized by either increased spatial resolving power or superior motion perception. The deep-sea *Conocara* spp. appear to have evolved an efficient way of optimizing both strategies, where large foveate eyes and large tecta may mediate increased spatial resolving power (Fernald 1988) and motion sensitivity (Guthrie 1990), particularly useful for tracking moving bioluminescent prey.

We wish to thank Michael Archer of the Department of Zoology, The University of Western Australia, for his expert technical assistance. We also thank the Natural Environment Research Council, the Master and Crew of the RRS *Challenger* (cruises 91 and 122) and RRS *Discovery* (cruise 204) and the remainder of the I-team. This research was funded by an Alexander von Humboldt Fellowship (S.P.C.), the National Health and Medical Research Council and Australian Research Council (S.P.C.) and the Deutsche Forschungs-gemeinschaft (H.-J.W.).

REFERENCES

Collin, S. P. 1999 Behavioural ecology and retinal cell topography. In *Adaptive mechanisms in the ecology of vision* (ed. S. N. Archer, M. B. A. Djamgoz, E. R. Loew, J. C. Partridge & S. Vallerga), pp. 509–535. London: Kluwer Academic.

Collin, S. P. & Collin, H. B. 1988 Topographic analysis of the retinal ganglion cell layer and optic nerve in the sandlance *Limnichthyes fasciatus* (Creeiidae, Perciformes). *J. Comp. Neurol.* **278**, 226–241.

Collin, S. P. & Collin, H. B. 1999 The foveal photoreceptor mosaic in the pipefish, *Corythoichthys paxtoni* (Syngnathidae, Teleostei). *Histol. Histopathol.* **14**, 369–382.

Collin, S. P. & Partridge, J. C. 1996 Retinal specializations in the eyes of deep-sea teleosts. *J. Fish Biol.* **49**(Suppl.A), 157–174.

Collin, S. P. & Pettigrew, J. D. 1988 Retinal topography in reef teleosts. I. Some species with well-developed areae but poorly developed streaks. *Brain Behav. Evol.* **31**, 269–282.

Collin, S. P. & Pettigrew, J. D. 1989 Quantitative comparison of the limits on visual spatial resolution set by the ganglion cell layer in twelve species of reef teleosts. *Brain Behav. Evol.* **34**, 184–192.

Collin, S. P., Hoskins, R. V. & Partridge, J. C. 1998 Seven retinal specializations in the tubular eye of the deep-sea pearleye, *Scopelarchus michaelsarsi*: a case study in visual optimization. *Brain Behav. Evol.* **51**, 291–314.

Döving, K. B. & Gemne, G. 1965 Electrophysiological and histological properties of the olfactory tract of the burbot (*Lota lota* L.). *J. Neurophysiol.* **28**, 139–153.

Easter Jr, S. S., Bratton, B. & Scherer, S. S. 1984 Growth-related order of the retinal fiber layer in goldfish. *J. Neurosci.* **4**, 2173–2190.

Fernald, R. D. 1988 Aquatic adaptations in fish eyes. In *Sensory biology of aquatic animals* (ed. J. Atema, R. R. Fay, A. N. Popper & W. N. Tavolga), pp. 339–363. New York: Springer.

Guthrie, D. M. 1990 The physiology of the teleost optic tectum. In *The visual system of fish* (ed. R. H. Douglas & M. B. A. Djamgoz), pp. 279–343. London: Chapman & Hall.

Huber, R. & Rylander, M. K. 1991 Quantitative histological studies of the optic tectum in six species of *Notropis* and *Cyprinella* (Cyprinidiae, Teleostei). *J. Hirnforsch.* **32**, 309–316.

Huber, R., Van Staaden, M. J., Kaufman, L. S. & Liem, K. L. 1997 Microhabitat use, trophic patterns, and the evolution of brain structure in African cichlids. *Brain Behav. Evol.* **50**, 167–182.

Kotrschal, K. & Palzenberger, M. 1992 Neuroecology of cyprinids: comparative, quantitative histology reveals diverse brain patterns. *Environ. Biol. Fish.* **33**, 135–152.

Locket, N. A. 1985 The multiple bank fovea of *Bajacalifornia drakei*, an alepocephalid deep-sea teleost. *Proc. R. Soc. Lond.* B **224**, 7–22.

Locket, N. A. 1992 Problems of deep foveas. *Aust. NZ J. Ophthamol.* **20**, 281–295.

Nicol, J. A. C. 1989 *The eyes of fishes.* Oxford Science Publications. Oxford, UK: Clarendon Press.

Schwassmann, H. O. 1975 Central projections of the retina and vision. In *Vision in fishes. New approaches in research* (ed. M. A. Ali), pp. 113–126. New York: Plenum Press.

Tamura, T. 1957 A study of visual perception in fish, especially on resolving power and accommodation. *Bull. Jap. Soc. Sci. Fish* **22**, 536–557.

Wagner, H.-J., Fröhlich, E., Negishi, K. & Collin, S. P. 1998 The eyes of deep-sea fish. II. Functional morphology of the retina. *Prog. Ret. Eye Res.* **17**, 637–685.

PHILOSOPHICAL TRANSACTIONS OF THE ROYAL SOCIETY B BIOLOGICAL SCIENCES